Influence of some additives on Cu layers formation in underpotential and overpotential regions in acidic $CuSO_4$ solutions. 7. Nucleation and growth of Cu onto smooth polycrystalline Pt and onto Se-modified Pt

Antanas Steponavičius, Dijana Šimkūnaitė, Svetlana Lichušina and Vidmantas Kapočius

Institute of Chemistry,
A. Goštauto 9,
LT-2600 Vilnius, Lithuania

The initial stages of Cu deposition from 0.5 M H_2SO_4 +0.1 M $CuSO_4$ solution onto a bare or selenium-modified smooth polycrystalline Pt electrode have been studied by cyclic voltammetry and potentiostatic step techniques. It has been established that at potentials more negative than the equilibrium potential for the couple Cu/Cu^{2+} the initial stages of Cu deposition onto the bare Pt electrode occur likely through the instantaneous 3D nucleation and growth under diffusion control model by Scharifker and Hills, taking into account the different numbers of formed nuclei in different parts of electrode surface. It was assumed that the area of such two parts might be of macroscopic dimensions rather than of microscopic or atomic ones. Modification of Pt surface by adsorbed selenium caused some changes in the mode of Cu deposition. For deposition of Cu on the Se-modified Pt electrode, the current–time characteristics can also be interpreted on the basis of a model involving instantaneous nucleation on both parts of electrode surface, as with bare Pt. However, the Cu nucleation process on the rest part corresponding likely to a Se-covered electrode surface seems to be rather negligible. Though the first part of the electrode is larger, the number of formed Cu nuclei per cm^2 is smaller as compared with bare Pt. Open-circuit Pt potential relaxation experiments conducted in the supporting 0.5 M H_2SO_4 solution have shown a somewhat different time response of potential for bare Pt and for Se-modified Pt electrodes.

Key words: Cu deposition, additives, influence

INTRODUCTION

Although considerable effort has been made recently to investigate the initial stages of copper electrodeposition in acidic Cu^{2+} solutions without [1–7] or with some additives [8–10], the conclusions on this matter are not always the same, especially relative to the mechanism and its dependence on the nature and state of a foreign substrate (*S*) surface. For example, it has been reported that experimental data fit very close the progressive 3D Cu nucleation and growth mechanism for vitreous carbon [2], glassy carbon [7], Au(111) [4] and smooth polycrystalline Pt [5] substrates. At the same time, the latter observation is in marked contrast to an other published work in which it has been shown that the Cu deposition quite likely fulfils the instantaneous 3D nucleation and growth mechanism in the entire time (*t*) window with a Pt electrode [3]. It is highly plausible that such a discrepancy may be caused by different experimental conditions, *e.g.* dissimilar concentration (*c*) of Cu^{2+}, pH, temperature and pretreatment of the electrode. A certain controversy has also been observed concerning the number of atoms in a critical cluster ($N_{crit.}$). Particularly, this parameter was reported to be close to zero on a vitreous carbon electrode [2], to 2–3 on an Au(111) electrode [4] or to *ca*.1 on a polycrystalline Pt electrode [5]. The effect of solution pH seems to be also imperfectly understood. Hence, a variation in the characteristics of the potentiostatic current–time transients applied conventionally for mechanistic and

kinetic analysis often interferes with an unambiguous understanding of the nucleation-growth phenomena.

Generally, the state of a foreign *S* surface was established to be very important for classifying the mechanism of deposition of not only Cu, but also of other metals (M) [11–13]. The state of *S* surface may be changed accidentally due to various contingencies or, for the most part, expediently. In the latter case, one of such ways is modification of a foreign *S* surface by the underpotential deposition (UPD) of M or by the formation of certain non-metallic adsorbed layers. If a metal bulk phase is formed on the top of an adsorbed layer deposited underpotentially, the conventional theories of electrocrystallization of M can be strictly applied.

On the other hand, it is of theoretical interest to investigate the initial stages of M deposition under conditions when a specified additive is present in the system under study. In this regard, some selenium and sulphur substances seem to be of primary interest. In particular, it has been shown that the Cu UPD onto a foreign M substrate changes upon the addition of sulphur-containing additive interacting with this substrate and probably taking place in redox reactions [14–20]. It has been recognized that the specific pattern of cyclic voltammogram (CV) characteristic of the Cu UPD on a bare single-crystal or on a bare polycrystalline Pt electrode disappears, and a new one becomes generated under the influence of some S-containing adsorbates. This new pattern was shown to be mainly associated with appearance of a new current peak shifted toward more negative potentials relative to the UPD peaks that are observed in solutions without any additive. It is only recently that the Cu UPD onto a polycrystalline Pt electrode from an acidic $CuSO_4$ solution containing a Se compound, selenite, has been started to be studied as well [21–23]. Taking into consideration that reduction of adsorbed S- or Se-substances being initially solution constituents may result in a certain modification of a Pt surface with S [24–28] or Se [29, 30] species, it is of theoretical importance to apply a Pt electrode modified by these elements.

The object of this work was chronoamperometric investigation of the initial stages of Cu electrodeposition onto the Se-modified smooth polycrystalline Pt electrode from an acidic $CuSO_4$ solution. Taking into account a possible variation in the competitive adsorption of different constituents of solution with a change of the electrode surface state, our second aim was thus to study the time response of potential for the bare Pt and Se-modified Pt electrodes under open-circuit conditions in a supporting H_2SO_4 solution.

EXPERIMENTAL

The working solution was 0.1 M $CuSO_4$ + 0.5 M H_2SO_4. The solution was prepared from doubly distilled water, salt $CuSO_4 \cdot 5H_2O$ (Fluka) preheated for 4 h at 400 °C and highest purity H_2SO_4 (Russia). H_2SeO_3 (99.999% purity) (Aldrich) was used for preparation of solution applied for modification of Pt electrode. Prior to each experiment, the working solution was deaerated with purified Ar gas for 0.5 h.

All experiments were performed at 20 ± 0.1 °C in a conventional three electrode thermostated electrochemical cell. The working electrode was a vertical disc made from a polycrystalline Pt foil (99.99% purity). The geometric area of the working electrode was 1 cm^2. The counter electrode was a Pt sheet of *ca*. 4 cm^2 in area. The reference electrode was a Ag/AgCl/KCl(sat.) electrode. In the text, all potentials (*E*) were recalculated with respect to the standard hydrogen electrode (SHE).

The real electrode surface area was determined from the hydrogen adsorption *i*/*E* profile recorded at 50 mV s^{-1} in 0.5 M H_2SO_4 solution and taking a specific charge of 210 μC for the complete coverage of 1 cm^2 of polycrystalline Pt by H_{ads}, as reported in [31]. The roughness factor (*f*) was obtained to be 1.75 ± 0.05. All currents (*i*) and charges (*Q*) in the text are recorded as current densities (*I*) and charge densities with respect to the geometric area of the electrode.

The pre-treatment of the working electrode prior to modification was described in detail elsewhere [19, 23, 32]. The selenium-modified Pt electrode was prepared by adsorption following a procedure described in [32]. The clean Pt electrode was allowed to stand at an open-circuit potential (OCP) in aqueous 2 mM H_2SeO_3 solution for 30 s. The characterization of the Se-modified electrode was carried out as in [32]. The coverage by Se (θ_{Se}) was found to equal 0.38 ± 0.05. Once prepared, the modified Pt electrode was thoroughly rinsed with doubly distilled water and, under a protection of a droplet of water, was transferred immediately to another cell for electrochemical measurements.

Chronoamperometric measurements were carried out using a PI 50–1 potentiostat interfaced through a home-made analogue to digital converter with a PC (Siemens), and a PR-8 programmer. The *I*/*t* traces were recorded starting with $E_{start.}$ = +0.35, +0.80, +1.00 or +1.20 V (all being in the *E* range positive of the E_{eq} for the couple Cu/Cu^{2+}), at which the electrode was held for 2 min, to various E_{dep} situated in the Cu overpotential deposition (OPD) region. The experimental data acquisition was in a numerical form with time resolution 50 ms per point.

After such experiments, the electrode was first held at E = +0.8 V in the same solution to remove completely the Cu deposit and then was cycled between +1.5 and +0.05 V in 0.5 M H_2SO_4 solution at 50 mV s^{-1} to dissolve oxidatively the selenium adlayer. For each E step experiment a freshly modified Pt electrode was used.

Separate experiments were also designed to check whether the selenium adlayer remained unchanged on reduction during a prescribed potential step. In order to gain such an evidence, the Cu deposit was dissolved anodically in the working solution at E = +0.8 V as mentioned above and then, after rinsing, the electrode was transferred into 0.5 M H_2SO_4 solution in which E was scanned at 50 mV s^{-1} from *ca.* +0.80 V to less positive values. The presence of selenium adlayer was assumed to be proved by a decrease of hydrogen adsorption. It was found that the voltammetric response in the hydrogen adatom potential range was almost the same as that recorded for the fresh Se-modified Pt electrode.

In some instances, a time response of the bare or modified Pt electrode potential in the supporting 0.5 M H_2SO_4 solution was examined after potentiostatic polarization at E_p = +0.050, +0.150 or +0.290 V for different time (t_E) followed by an opening of a potentiostat electronic circuit. These experiments were conducted using the equipment mentioned above.

RESULTS AND DISCUSSION

1. Time response of potential of the bare Pt and the selenium-modified Pt electrodes in 0.5 M H_2SO_4 solution

There has been recently a growing interest in obtaining and studying modified electrodes prepared by attaching various species to the surface of a conducting substrate. As mentioned above, one method for preparing modified electrodes is that such an attachment is made through irreversible adsorption. Such a method was applied in our study.

Taking into consideration a competitive adsorption of various kinds of adsorbate onto Pt (for hydrogen and sulphate/bisulphate adsorption see, *e.g.*, reviews [33–35] and a brief review of more recent studies presented in [36]) and also a possible complication in the understanding of the overall reaction due to these adsorption phenomena, the change in the surface state of the Pt electrode used here was simulated in some sense, following the procedure described in [37].

From the parallelism between the time responses of E of Pt(111) and of *in-situ* IRAS at this electrode in 0.5 M H_2SO_4 solution, the change in the surface state of the electrode was explained earlier [37] as follows. It has been established that when the Pt(111) electrode is kept at E_p = +0.05 V, atomic hydrogen, neutral H_2O and H_3O^+ molecules are forced to the surface of the electrode. After switching off this E_p, the amounts of atomic hydrogen and neutral water molecules are reduced, whereas that of H_3O^+ increases according to [37]:

$$H_{ad} + H_2O_{ad} \rightarrow H_3O^+_{ad} + e, \qquad (1)$$

resulting in an E increase (under the conditions of the study cited, around +0.3 to +0.4 V). Then, HSO_4^- ions start to be coadsorbed with H_3O^+. This increases E of Pt(111) remarkably until around +0.6 to +0.7 V.

The spontaneous increase in E established in [37] also correlates well with the observations of other authors [38] who investigated the adsorption of HSO_4^- and SO_4^{2-} on Pt substrate in 0.05 M H_2SO_4 solution, using EQCM and CV techniques. It has been estimated that the adsorption of HSO_4^- can commence even at E corresponding to deposition of hydrogen, and that the upper limit of coverage of HSO_4^- on Pt at +0.8 V amounts up to 0.15.

Examination of the change of E of the Pt electrode as a function of time (t) under open-circuit conditions in 0.5 M H_2SO_4 solution after preceding setting the potential at various values (specifically, E_p = +0.29, +0.15 or +0.05 V) showed that the time response of E of bare Pt or Se-modified Pt was markedly dependent on such parameters of prepolarization as E_p and t_E (Figs. 1–4). Hence, the explanation given in [37] seems to be sufficiently workable for our case as well.

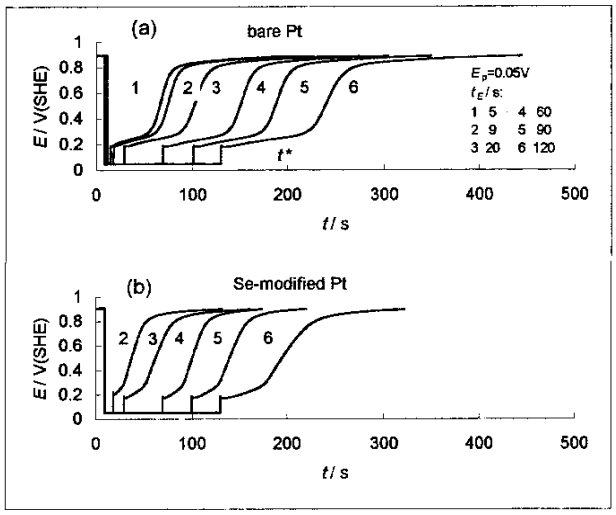

Fig. 1. Time response of potential of bare polycrystalline Pt (*a*) and Se-modified Pt (*b*) electrodes in 0.5 M H_2SO_4 solution under open-circuit conditions after immersion of electrodes at polarization potential E_p for time t_E

As can be seen from the E *vs*. t plots displayed in Fig. 1*a*, in the case when E_p of the Pt electrode is initially set at +0.05 V (where no anion adsorption occurs), the subsequent E change occurs differently, depending on time window, *viz*. E increases first gradually and then rapidly after a lapse of certain time t^*, in a good qualitative agreement with observations in [37]. A rather similar pattern was also obtained for the Se-modified Pt electrode (Fig. 1*b*). For the electrodes of both types, the duration of t^* increases with time of their holding (t_E) at the chosen value of E_p. The relationship between these quantities may be represented as an n-power function (Fig. 2). As expected, the larger t^* were obtained with bare Pt compared with Se-modified Pt. Moreover, the power n for the latter electrode was obtained to be about twice as large as that for bare Pt. In all probability, the modification of Pt electrode used here transforms the experimental t^* *vs*. t_E relationship (Fig. 2) due to two effects occurring simultaneously, namely, the blocking effect, on the one hand, and the action of selenium as a modifier of metal surface electronic properties resulting in an enhancement of the sensitivity of hydrogen adsorption to the duration of holding Pt at a chosen value of E_p, on the other hand.

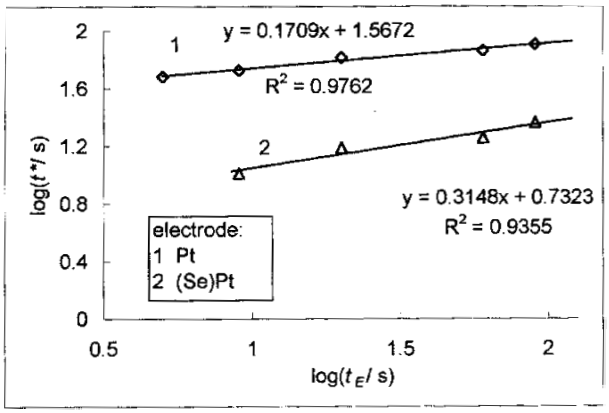

Fig. 2. Log-log dependence of the time t^*, corresponding to a gradual change of potential in Fig. 1, on the time t_E, corresponding to the length of immersion of electrode at E_p = +0.050 V

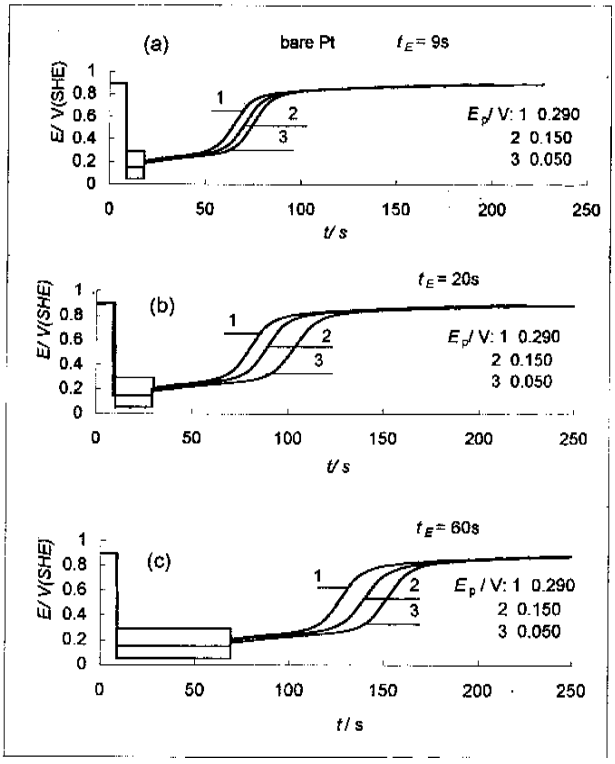

Fig. 3. Time response of potential of bare Pt electrode in 0.5 M H_2SO_4 solution under open-circuit conditions after immersion of the electrode at different E_p for t_E = 9 (*a*), 20 (*b*) or 60 s (*c*)

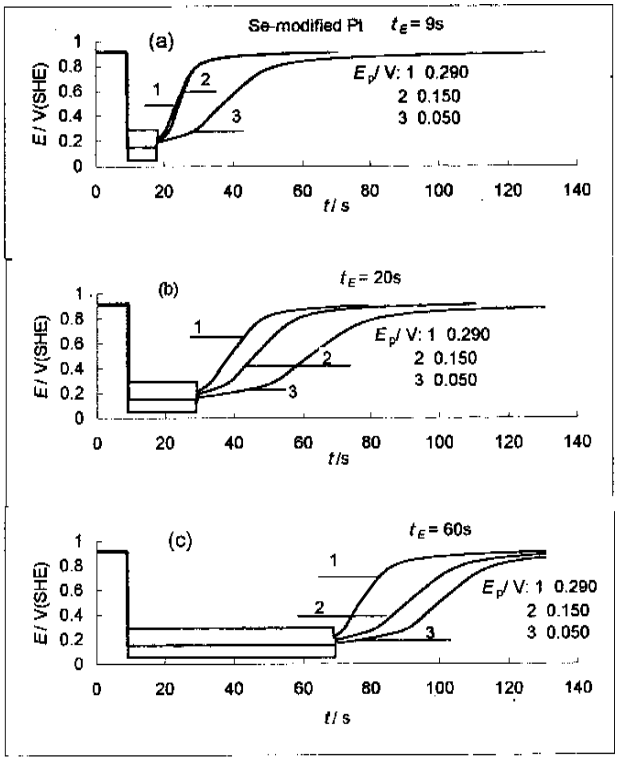

Fig. 4. The same as in Fig. 3, but for the Se-modified Pt electrode

As one would expect, Figs. 3 and 4 show that the quantity t^* which should be associated mainly with the amount of adsorbed hydrogen, decreases with increasing the magnitude of the prepolarization potential E_p.

2. Overpotential deposition of Cu

2.1 ***Voltammetry.*** Characteristic voltammograms recorded for Cu deposition and dissolution over the E region covering both the UPD and OPD ranges at the potential scan rate of 2 mV s^{-1} from E_{start} to

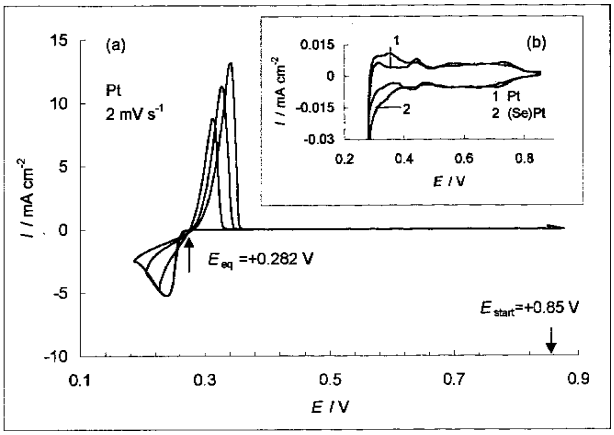

Fig. 5. Cyclic voltammograms for Cu deposition/dissolution in 0.5 M H_2SO_4 + 0.1 M $CuSO_4$ solution recorded from E_{start} to different lower limits of sweeps (*a*) and the same as in (*a*), but only in the UPD potential region (*b*). Curves in (*a*) are background-corrected, whereas in (*b*) they are presented as recorded

different lower limits are shown in Fig. 5. In all cases single sweeps were applied. No significant changes of the *i*/*E* curves were observed in the OPD region when the bare Pt electrode was replaced by the Se-modified one (each curve was recorded using a freshly modified Pt electrode). An exception was the *E* region of the formation and ionization of Cu adlayer (Fig. 5*b*). The regularities of Cu adlayer deposition/dissolution for the Pt electrode of both types have already been discussed in detail [32].

A closer analysis of CVs also shows that they display the hysteresis loop in the cathodic half-cycle (Fig. 5 and in an enlarged scale in Fig. 6). Such a hysteresis loop was found to be indicative of a nucleation/growth process [39]. From the almost linear descending branch of the cathodic curve (Fig. 6), one can also assume that the growth of the created hemispherical nuclei should be "reversible", in accordance with considerations in [39]. A similar response was already observed for Cu deposition onto the polycrystalline Pt electrode from sulphate solution containing Cu^{2+} and Ag^+ in the event when reverse *E* was more positive than the value of the half-peak potential of voltammetric Cu wave [40].

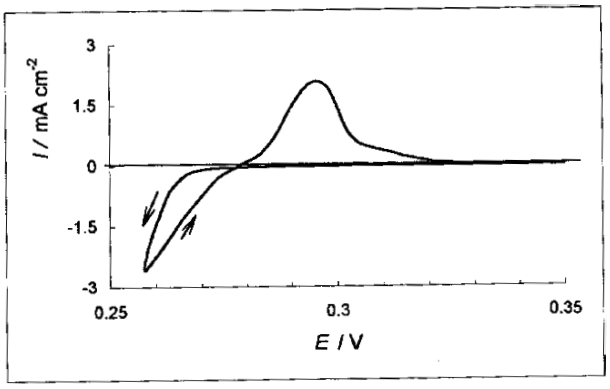

Fig. 6. The same as in Fig. 5*a* in an enlarged scale when the reverse potential was +0.257 V

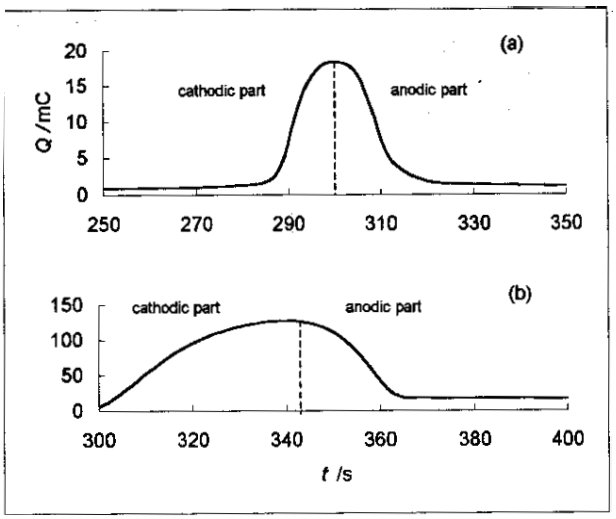

Fig. 7. Variation of charges obtained by integrating the respective voltammetric waves of the cathodic (an increase in the amount of deposited metal) and anodic (a decrease in the amount of deposited metal due to a subsequent dissolution) half-cycles with time: *a* – according to the data from Fig. 6, *b* – from the data in Fig. 5*a* when the reverse potential was +0.227 V

The other characteristic feature of CV displayed in Fig. 6 is that the charges (*Q*) obtained by integrating the respective waves of the cathodic and anodic half-cycles (in other words, the quantities related to the amount of deposited metal and to a decrease in this amount with time during anodic dissolution) are almost symmetric about the y-axis at the time when the current changes its sign (Fig. 7*a*). From the value of *Q* (Fig. 7*a*) and taking into account the roughness factor, it follows that the amount of deposited Cu (Fig. 6) corresponds to approximately 20 monolayers. In this calculation, it was assumed that the charge density corresponding to a monolayer of Cu equals 0.49 mC cm^{-2}. However, this symmetry was broken when a thicker Cu layer was deposited and dissoluted subsequently. One can see in Fig. 7*b* that the rate of Cu dissolution defined as d*Q*/d*t* is markedly higher as compared with the previous case. Therefore, among the differences in the properties related to the thin and to the thicker Cu layers, the dissimilar anodic behaviour can also be listed.

2.2 ***Chronoamperometry.*** *(a) Bare Pt electrode.* Typical sets of current–time transients for Cu OPD on the bare Pt electrode from 0.5 M H_2SO_4 + 0.1 M $CuSO_4$ solution are shown in Figs. 8*a*, 9*a*. Rather similar transients were also obtained starting from

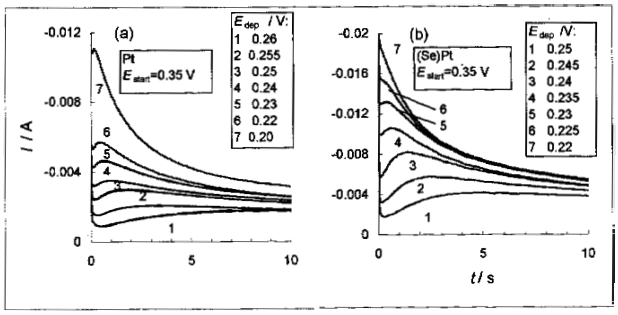

Fig. 8. Potentiostatic current transients for Cu deposition onto the bare polycrystalline Pt electrode (*a*) and onto the Se-modified Pt electrode (*b*) in 0.5 M H_2SO_4 + 0.1 M $CuSO_4$ solution. The starting potential E_{start} = +0.35 V. The values of the E_{dep} up to which the potential was cathodically stepped, are indicated in Figure. The equilibrium potential for the couple Cu/Cu^{2+} $E_{eq.}$ = +0.282 V

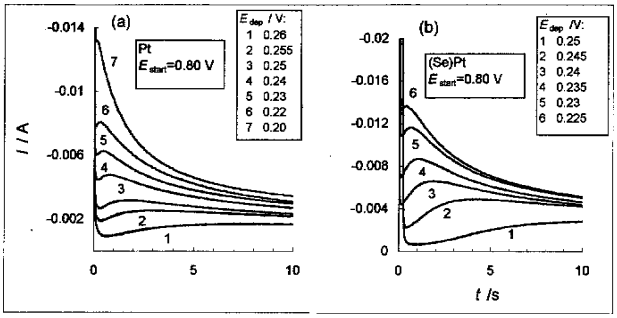

Fig. 9. The same as in Fig. 8, but for E_{start} = +0.8 V

+1.0 and +1.2 V. In most cases, these transients had a shape which was rather close to that expected for a polynuclear 3D nucleation with growth under diffusion control model described by Scharifker and Hills [41]. In a very short time, a sharp current peak due to double layer charging is observed (a certain contribution of some parasitic processes, most likely related to Cu^+ and to the adsorption of the first Cu monolayer should also be admitted). In the succeeding part of the transient, I rises to a maximum (I_{max}) at t_{max} and, at $t>t_{max}$, all I/t curves tend to merge into one, reflecting the linear diffusion limitations to become prevailing.

For 3D nucleation/growth with diffusion control after the potential step into the OPD region, two limiting cases are predicted, according to the theory by Scharifker and Hills [41]. At high nucleation rates (when all the nuclei are immediately created and their number remains constant during the growth process), so-called instantaneous 3D nucleation, the whole I/t profile can be described by equation:

$$I(t) = (zFD^{1/2}c/(\pi t)^{1/2})[1-\exp(-\pi k_e DN\, t)], \quad (2)$$

where $I(t)$ is the current normalized by the geometric area of the electrode surface, N is the total number of the created nuclei (in cm^{-2}), k_e is the numerical constant determined by the properties of material:

$$k_e = (8\pi cM/\rho)^{1/2}, \quad (3)$$

M and ρ are the molar mass and the density of the deposited metal, respectively, zF is the molar charge of the electrodepositing species, D and c are the diffusion coefficient and bulk concentration (in mol cm^{-3}) of the metal ions to be deposited, respectively.

For a continuous formation of new nuclei during the entire t window before overlap of diffusion hemispheres around the growing nuclei (resulting in Cu clusters of different sizes), so-called progressive 3D nucleation, the current transients are described by equation

$$I(t) = (zFD^{1/2}c/(\pi t)^{1/2})\,[1-\exp(-aN_o\pi k_e' Dt^2/2)], \quad (4)$$

where N_o is the density of S active sites (in cm^{-2}), a is the steady-state nucleation rate constant per site, aN_o is the nucleation rate, k_e' is again the numerical constant given by:

$$k_e' = (4/3)(8\pi cM/\rho^{1/2} \quad (5)$$

In order to characterize the 3D nucleation/growth process, the current transients can be plotted as reduced variables $(I/I_{max})^2$ *vs.* t/t_{max} [41] – for instantaneous nucleation:

$$(I/I_{max})^2 = 1.9542(t/t_{max})^{-1}\{1-\exp[-1.2564(t/t_{max})]\}^2, \quad (6)$$

and for progressive nucleation:

$$(I/I_{max})^2 = 1.2254(t/t_{max})^{-1}\{1-\exp[-2.3367(t/t_{max})^2]\}^2. \quad (7)$$

The typical experimental $(I/I_{max})^2$ *vs.* (t/t_{max}) plots together with the predicted ones are presented in Fig. 10. From these plots it can be concluded that Cu deposition onto the bare polycrystalline Pt electrode from 0.5 M H_2SO_4 + 0.1 M $CuSO_4$ solution likely fulfils the instantaneous 3D nucleation and diffusion-controlled growth mechanism by Scharifker and Hills [41] in the entire t window used for our experiments, in agreement with the data in [3].

On the other hand, it is important to emphasize here that some features of the current transients (Figs. 8, 9) and of the experimental $(I/I_{max})^2$ *vs.* t/t_{max} plots (Fig. 10) do not satisfy the requirements of the theory [41, 42]. For example, the values of N calculated for the same E step from the expressions

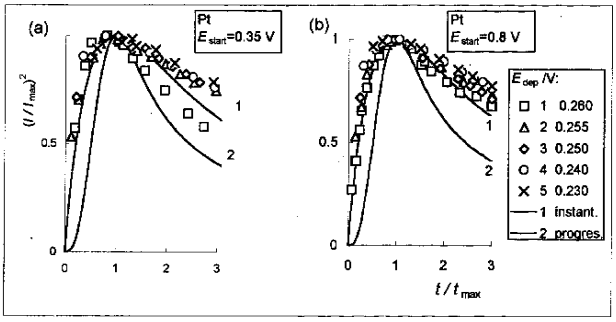

Fig. 10. Reduced-variable plot of transients for bare Pt electrode (from Figs. 8, 9). E_{start} and E_{dep} are indicated in Figure. Calculated curves for instantaneous (*1*) and progressive (*2*) 3D nucleation with diffusion-controlled growth model according to [41] are also shown. $E_{eq.}$ = +0.282 V

for t_{max} and I_{max} for the instantaneous 3D nucleation and diffusion-controlled growth mechanism [41, 42]:

$$t_{max} = 1.2564/N\pi k_e D, \quad (8)$$

$$I_{max} = 0.6382zFDc(k_e N)^{1/2} \quad (9)$$

at D for Cu^{2+} ion taken as $5.6\cdot10^{-6}$ cm^2 s^{-1} (Ref. 20 in [43]) and k_e = 0.134 were obtained to be somewhat different. Further, although the value of product $I^2_{max}\cdot t_{max}$ should be constant with varying η_c, as predicted in [41]:

$$I^2_{max}\cdot t_{max} = 0.1629(zFC)^2D, \quad (10)$$

it was obtained that, under conditions of our experiments, this parameter varied rather indefinitely in the intervals $1.42\cdot10^{-5}$ to $3.67\cdot10^{-5}$ at $E_{start.}$ = 0.35 V and $1.93\cdot10^{-5}$ to $2.9\cdot10^{-5}$ A^{2}s at $E_{start.}$ = 0.8 V for the bare Pt electrode. Moreover, the average values of the product $I^2_{max}\cdot t_{max}$ ($1.814\cdot10^{-5}$ and $2.37\cdot10^{-5}$, respectively) gave D for Cu^{2+} ion being one order of magnitude less than the reliable values for this parameter presented in the literature (see, *e.g.*, a review paper [43]). Finally, the falling parts of the $(I/I_{max})^2$ *vs.* t/t_{max} plots (Fig. 10) are shifted above the theoretical plot (such deviations from the theoretical lines after the maximum have already been observed in experimental studies [8, 44–46] and have been explained by different physical reasons).

Some reasons may be considered to be responsible for the observations related to the current transients. The most plausible reason, in our opinion, may be as follows. Because the 3D nucleation and growth under diffusion control model [41, 42] should imply the nucleation stages proceeding onto highly homogeneous surfaces of inert electrodes, one can assume that the observations mentioned above are associated with a strong influence of inhomogeneity of the electrode surface. Such an assumption can be supported, particularly, by rather numerous notes in the literature (see, *e.g.*, [47–53]) that both the surface topography and the variation in the energetic state due to various crystallographic defects in a very top layer of an inert electrode may have a pronounced effect on the peculiarities of electrochemical formation of the new phase. Our concept is based firstly on an assumption of a different number of nuclei (N) which can be formed in separate zones of Pt electrode surface (N_1) and in the rest of Pt surface (N_2), provided the instantaneous 3D nucleation and diffusion-controlled growth model is case. These zones are further assumed to be of macroscopic dimensions rather than of microscopic or atomic ones. Such a presence of separate zones may be originated, in our minds, from a certain accumulation of the surface defects compared with their more random distribution in the rest of Pt electrode surface.

The proposed concept can be illustrated in a following way. The instantaneous 3D nucleation with diffusion-controlled growth model for Cu deposition onto the bare Pt electrode is further assumed to be the case, as stated above. Then, for simplicity's sake, one can assume that the whole area of Pt electrode surface consists of two main parts. The first part can be defined as a sum of the separate zones in which the number of formed nuclei is actually the same, say, N_1 in cm^{-2}. The second part, then, becomes equal to the rest of surface area with the number of instantaneously formed nuclei $N_2 \ll N_1$. In terms of the theory of Scharifker and Hills [41], the parameter N_1 can be

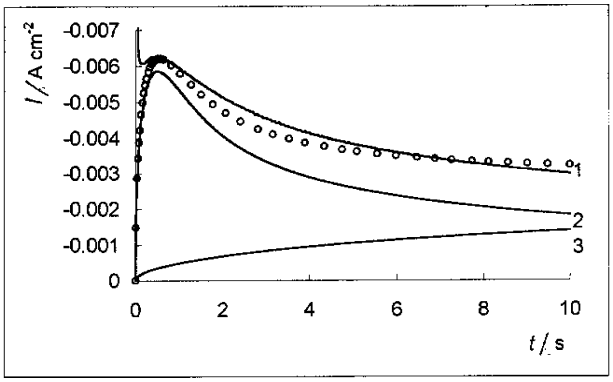

Fig. 11. Potentiostatic current transients for Cu deposition onto bare polycrystalline Pt electrode in 0.5 M H_2SO_4 +0.1 M $CuSO_4$ solution. Full lines: *1* – experimental curve (from Fig. 9*a*, curve *5*); *2* – calculated using Eq. (11) at θ = 0.224 and $N_1 = 1.066\cdot10^6$ cm^{-2}; *3* – obtained by subtraction of curve *2* from curve *1* (exluding the sharp current peak at a very short time). Curve denoted by open circles – obtained using Eq. (12) at θ = 0.224, $N_1 = 1.066\cdot10^6$ cm^{-2} and $N_2 = 10.6\cdot10^3$ cm^{-2}. E_{start} = +0.80 V, $E_{eq.}$ = +0.282 V, E_{dep} = +0.23 V

estimated from t_{max} which is independent of the working area of an electrode, provided current density is used instead of current. For the case of the bare polycrystalline Pt electrode at $E_{start.} = +0.80$ V, $E_{dep} = +0.23$ V (Fig. 9, curve *5* and Fig. 11, curve *1*), using Eq. (8) and $D = 5.6 \cdot 10^{-6}$ cm^2 s^{-1}, N_1 was found to be equal to $1.066 \cdot 10^6$ cm^{-2}. Since $c = 10^{-4}$ mol cm^{-3}, $k_e = 0.143$, and $N_1 = 1.066 \cdot 10^6$ cm^{-2}, the theoretical value of I_{max} calculated from Eq. (9) was obtained to be equal to $2.607 \cdot 10^{-2}$ A (this value should be expected if the whole area of Pt surface is suitable for the formation of N_1 nuclei). Then, the fractional surface area θ corresponding to the first part of the Pt electrode surface was estimated as a ratio $\theta = I_{max,exp}/I_{max,calc}$. It was found that θ = 0.224. Further, introducing the parameter θ in the expression for the current transient to the whole electrode surface, in Eq. (2), one obtains an expression related only to the first part of the working electrode surface:

$$I(t)_1 = [zFD^{1/2}c/(\pi t)^{1/2}] \cdot \theta \cdot [1-\exp(-\pi k_e D N_1 t)]. \quad (11)$$

The current transient calculated using Eq. (11) is shown in Fig. 11 (curve *2*).

Subtracting curve *2* from curve *1* (Fig. 11), one obtains the curve $I(t)_2$ (curve *3*) which represents not only a simple difference between these curves, but also, in our mind, an increase in current due to the growth of the nuclei formed instantaneously onto the rest part of the Pt electrode surface (1–θ). The current transient $I(t)_2$ obtained by this means can be used to estimate the second number of the formed nuclei, N_2. Taking the value of I at a selected t, say, at $t = 7$ s, one obtains that $N_2 = 10.6 \cdot 10^3$ cm^{-2}. Using this value of N_2, the expression for the current transient $I(t)_2$ suitable for the further calculations can be easily obtained.

Finally, in accordance with our concept, *i.e.* taking $I(t)$ as a sum of $I(t)_1 + I(t)_2$, the expression for the current transient which accounts for Cu deposition through the instantaneous 3D nucleation and diffusion-controlled growth model in both parts of the surface of the working Pt electrode with different values of N can be derived:

$$I(t) = [zFD^{1/2}c/(\pi t)^{1/2}] \cdot [1-\theta \cdot \exp(-\pi k_e D N_1 t) + \theta \cdot \exp(-\pi k_e D N_2 t) - \exp(-\pi k_e D N_2 t)]. \quad (12)$$

The resulting current transient obtained using Eq. (12) is presented in Fig. 11 (the data are given as open circles). A comparison of the latter data with the experimental curve *1* strongly suggests that the proposed concept is sufficiently justified. A rather minor difference between the experimental and the calculated data seems to be connected with a factor that is as yet neglected in our considerations. Further investigations concerning this problem are in progress.

The other $I(t)$ curves recorded here with the bare polycrystalline Pt electrode can be analyzed in a similar way.

It must be realized that the formalism used to illustrate our concept involves a certain indefiniteness. In particular, the parameter N_1 was calculated from the experimental value of t_{max} under the assumption that instantaneous nucleation occurs uniformly on the whole surface of Pt. In the further considerations, it was refined that the whole working surface consisted of two parts. In our opinion, employment of t_{max} without a correction for presence of the second part of the surface may be rather justified provided $N_1 >> N_2$ (in this case, a contribution of the current related to the second part is rather negligible).

Besides, it is still not clear why the whole working surface consists of two (or even more) separate parts of macroscopic dimensions. In this connection it should be noted that an effect of various factors on the energetic state of the substrate surface and, consequently, on the kinetics and thermodynamics of electrochemical phase formation has already been studied rather extensively. Among such factors, conditions of pretreatment such as voltammetric procedure, temperature, etc. and physical processes such as UPD, anion specific adsorption, oxide formation/reduction, surface reorganization, etc. should be mentioned first (see, *e.g.*, [13, 47, 54–56]). In the present paper, the origin of a variation of energetic states of the separate parts of the working Pt electrode with respect to Cu nucleation was not considered in detail, but, in this context, one can suppose that such a state of Pt surface resulted mainly from the procedure of cycling applied during the pretreatment of polycrystalline Pt.

Continuing the treatment of the experimental chronoamperometric data in line with the proposed model, one can estimate the overpotential-dependences of N_1 and N_2. The relations derived only from Figs. 9*a* and 11 are illustrated in Fig. 12. The analogous relations for N_1 obtained here with the bare Pt electrode under various experimental conditions are also presented (Fig. 13). As can be seen, the calculated values of N_1 are practically independent of E_{start}. To our mind, this point is worth to be emphasized because the chosen values of E_{start}, namely, +0.80 and +0.35 V, are quite different with respect to the Cu UPD process [1, 3, 13, 20, 22, 53, 57–64]. So, it seems that the inhomogeneity of Pt surface as assumed above shows a stronger effect on the mode of Cu nucleation than the presence of Cu layer deposited underpotentially when the Pt electrode was

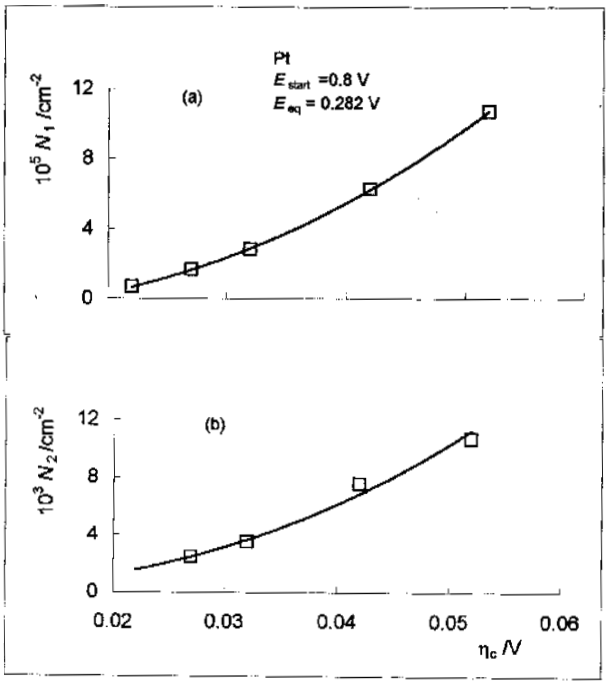

Fig. 12. Variation of the numbers of Cu nuclei formed instantaneously, N_1 and N_2, onto bare polycrystalline Pt in 0.5 M H_2SO_4 +0.1 M $CuSO_4$ solution with Cu overpotential. Calculation of N_1 and N_2 is described in the text

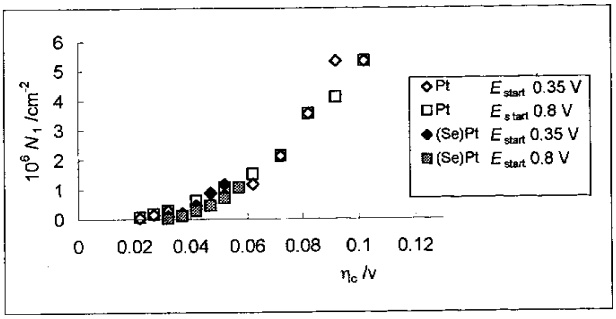

Fig. 13. Variation of the number of Cu nuclei formed instantaneously, N_1, onto bare polycrystalline Pt or onto Se-modified Pt in 0.5 M H_2SO_4 +0.1 M $CuSO_4$ solution with Cu overpotential and starting potential E_{start}

held at E_{start} = +0.35 V for 2 min before the E steps or its absence in the case of E_{start} = +0.80 V.

The proposed model was verified additionally by a correlation between the family of the experimental current transients recorded with the E steps to different E_{dep} and the calculated one. It can be seen from Fig. 14 that there is a good quantitative agreement between experiments and calculations.

(b) Se-modified Pt electrode. Measurements showed that the potentiostatic current transients recorded with the (Se)Pt electrode (Figs. 8*b*, 9*b*) were rather similar in the general shape to those in the previous case (Figs. 8*a*, 9*a*). Some differences observed were as follows. For the (Se)Pt electrode,

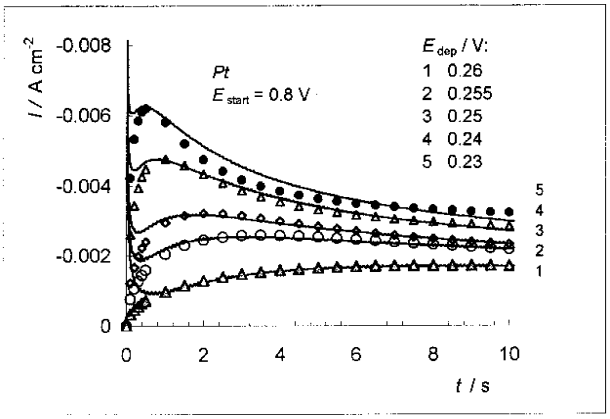

Fig. 14. Comparison of the experimental current transients taken from Fig. 9*a* (full lines) with the calculated ones (separate points). Calculation – according to Eq. (12)

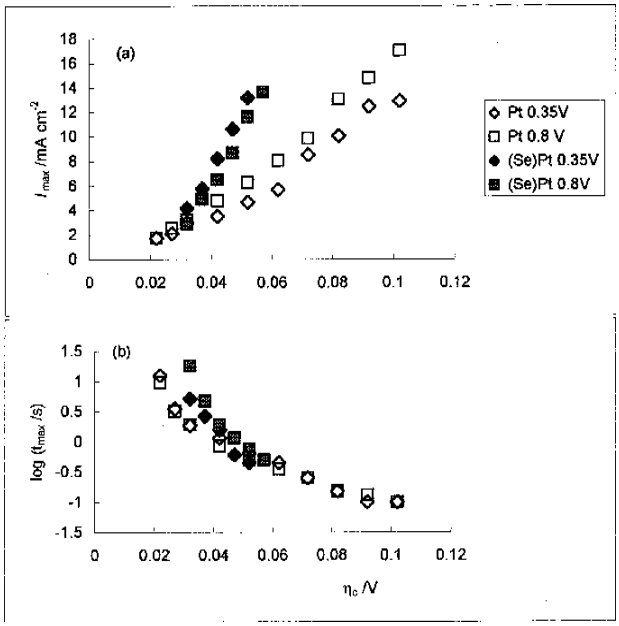

Fig. 15. Variation of the experimental values of I_{max} and t_{max} with overpotential and E_{start} for the bare Pt and Se-modified Pt electrodes (from the current transients displayed in Figs. 8, 9)

higher values of I_{max} were registered at the same E step, and the region of E_{dep} suitable for these measurements was narrower as compared with the bare Pt electrode (Fig. 15). Bearing in mind that Se compounds were found to cause Cu^{2+} discharge depolarization at Cu cathode [65–70], the changes in I_{max} and the width of E_{dep} interval observed here seem to be quite reasonable. The data obtained with the (Se)Pt electrode also showed that while t_{max} were significantly larger in the region of a more positive E_{dep}, this difference diminished at lower values of E_{dep}.

To make a quantitative assessment of the experimental current transients (Figs. 8*b*, 9*b*) to the theoretical requirements for instantaneous 3D nucleation [41, 42], the product $I^2_{max} \cdot t_{max}$ was analysed. It was found that, under conditions of our experiments, the values of this parameter were scattered to a somewhat lower degree as compared with the previous case, namely, they varied in the intervals $6.74 \cdot 10^{-5}$ to $9.44 \cdot 10^{-5}$ A^2s at E_{start} = 0.35 V and $8.03 \cdot 10^{-5}$ to $15.1 \cdot 10^{-5}$ A^2s at E_{start} = 0.80 V. Then, according to Eq. (10), the average values of the product $I^2_{max} \cdot t_{max}$ ($8.3 \cdot 10^{-5}$ and $10.4 \cdot 10^{-5}$, respectively) yielded D for Cu^{2+} ion being equal to $1.37 \cdot 10^{-6}$ and $1.72 \cdot 10^{-6}$ cm^2s^{-1}, respectively. Although these magnitudes of D for Cu^{2+} are larger than those obtained for the bare Pt electrode, they are still less than expected (*cf*. $5.6 \cdot 10^{-6}$ cm^2s^{-1}) by a factor of 4 or 3 (if one formally applies the expression for progressive nucleation, the calculated values of D larger only by *ca*. 60% will be obtained). These observations suggest that the instantaneous nucleation mechanism accepted for bare Pt appears to be somewhat complicated for (Se)Pt as well.

Figure 16 represents the data from Figs. 8*b*, 9*b* plotted in the coordinates $(I/I_{max})^2$ *vs*. t/t_{max} according to the theoretical model of 3D nucleation and diffusion-controlled growth of hemispherical clusters [41, 42]. As can be seen, the non-dimensional plots indicate that, at $t < t_{max}$, Cu deposition onto (Se)Pt formally follows the instantaneous nucleation model. However, at $t > t_{max}$, a certain part of the experimental data, namely those obtained at E_{start} = 0.80 V and more positive E_{dep} fall actually between the theoretical curves for instantaneous and progressive nucleation.

It should be noted that the general case, when the experimental chronoamperometric data fell between the theoretical curves $(I/I_{max})^2$ *vs*. (t/t_{max}) for instantaneous and progressive nucleation [41, 42] in the entire t interval, was already considered theoretically by Scharifker and Mostany [49] and by Tsakova and Milchev [50]. Besides, such a phenomenon was often observed in various systems, *e.g*., for deposition of Pb onto vitreous carbon [71], Hg onto Pt [50], Pt onto W [46], In onto glassy carbon and W in room temperature chloroaluminate molten salts [72]. It was shown that the experimental points can be located variously depending on the value of parameter α defined as a ratio $N_o \pi k_e D/A$, where N_o is the number density of active sites (cm^{-2}), k_e is the numerical constant (as in Eq. (3)), A is the nucleation rate per active site (s^{-1}) [49]. Then, the so-called "instantaneous" and "progressive" nucleation can be considered as extreme cases of a more general phenomenon of heterogeneous nucleation on a finite number of active sites on the electrode surface. These cases were assumed to correspond to the extreme situations of fast nucleation on a small number of active sites (small α) and slow nucleation on a large number of active sites (large α) [49].

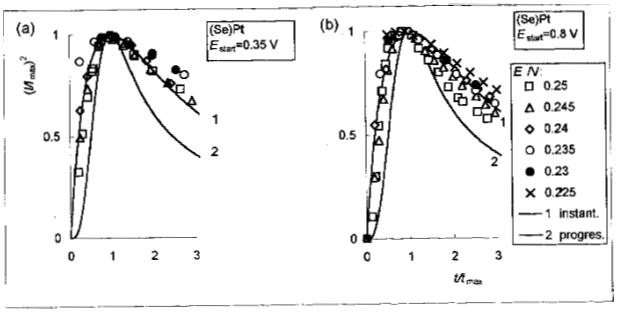

Fig. 16. Reduced-variable plot of the transients for the Se-modified Pt electrode (from Figs. 8, 9). E_{start} and E_{dep} are indicated in Figure. Calculated curves for instantaneous (*1*) and progressive (*2*) 3D nucleation with diffusion-controlled growth model according to [41] are also shown. E_{eq} = +0.282 V

The foregoing approach [49, 50] appears to be not applicable in the case of our interest because of a difference in the location of the experimental points at $t < t_{max}$, as pointed above. Then, one can again consider the model proposed here for describing the initial stages of Cu deposition onto the bare polycrystalline Pt electrode, *i.e*. assuming the presence of separate zones onto the surface of the working electrode with different activity with respect to nucleation. As in the previous case, one can further assume that the whole area of (Se)Pt surface consists of two main parts showing a different behaviour as the inert substrate.

In terms of theory [41], the parameter N_1 can be estimated from t_{max}. In this case, $t \le t_{max}$ were corrected for the induction time, t_{ind}. As is customary, for instantaneous nucleation t_{ind} can be obtained from the rising branches of the current transients plotted in the form of I^2 *vs*. t. In particular, it was obtained that t_{ind} was equal to 2 or 0.3 s at $E_{start.}$ = 0.80V and E_{dep} = 0.25 or 0.245V, respectively (as one would expect, the percentage part of t_{ind} in t_{max} decreased with applying a less positive E_{dep}). Using Eq. (8), N_1 was found to be equal to $3.7 \cdot 10^4$ or $12.5 \cdot 10^4$ cm^{-2} at these E_{dep}. Further, following the calculation procedure described above, the value of $I_{max,calc}$ was estimated from Eq. (9), and the fractional surface area θ as the ratio $I_{max,exp}/I_{max,calc}$ was evaluated. It was found that θ was 0.6 or 0.54, respectively. The current transients $I(t)$ calculated using Eq. (11) are shown in Fig. 17. As can be seen from the diagram, there is a good agreement between the experimental and calculated current transients providing support for the applicability of the proposed approach

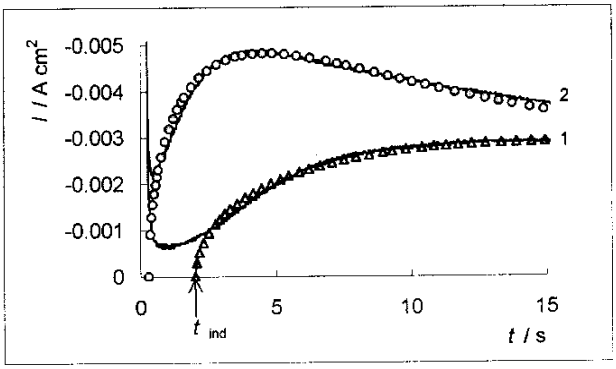

Fig. 17. Potentiostatic current transients for Cu deposition onto the Se-modified Pt electrode in 0.5 M H_2SO_4 +0.1 M $CuSO_4$ solution. Full lines: the experimental transients at E_{start} = +0.80 V and E_{dep} = +0.25 (*1*) or +0.245 V (*2*) (from Fig. 9*b*, curves *1* and *2*). Open points: calculated transients according Eq. (11) at θ = 0.6 or 0.54, N_1 = $3.7 \cdot 10^4$ or $12.5 \cdot 10^4$ cm^{-2}, respectively

and also indicating that the contribution of nucleation onto the rest area, (1-θ), of Se(Pt) is quite negligible.

The other current transients for the (Se)Pt electrode were analyzed in the same way.

Attention can be drawn to the fact that the rest of the area, 1-θ, at $E_{start.}$ = 0.8V is almost 0.4 at a lower η_c and approximately 0.5 at a higher η_c, showing a relatively good agreement with the experimental value of $\theta_{Se} \approx 0.38$. In our mind, this suggests that the active sites for Cu nucleation onto Se-covered Pt are holes or other structural defects in Se coverage where Cu nuclei are in direct contact with the original Pt surface. In this connection it should be noted that, on the basis of the assumption that Cu is not capable of displacing adsorbed selenium species from Pt surface, Cu UPD onto the Se-modified Pt electrode has been explained by formation of a mixed copper–selenium adlayer at higher underpotentials and deposition of a separate Cu layer onto Se-covered Pt in the range of small underpotentials [32]. Besides, an analogous assumption of direct contact between metal and covered substrate has already been made [55] considering the results of investigation of Hg deposition onto Pt [73] and of Pb onto Ag single crystal [48].

As is obvious from the data obtained, though the quantity θ for (Se)Pt was found to be larger than that for bare Pt, the number of active sites per cm^{-2} occupied by the formed stable Cu nuclei for the former substrate was about one order of magnitude less. Then, taking deposition of selenium species to occur onto the Pt surface sites of higher activity, the fractional surface area θ for (Se)Pt available for appreciable Cu nucleation can be correlated with the part of surface of bare Pt defined as 1-θ rather than with that defined as θ. It is apparent that such a correlation should not be rigorous,because the action of adsorbed selenium on the energetics of Pt surface is still not clearly understood [13, 79]. Particularly, this is evident from a comparison of N_2 in cm^{-2} for bare Pt with N_1 for (Se)Pt (*cf*. Fig. 12 *b* and Fig. 13) yielding that the latter quantity is larger, *e.g.*, at E_{start} = 0.80V and E_{dep} = 0.24 or 0.23V, by a factor of about 4.6 or 28, respectively.

CONCLUSIONS

It has been established that the initial stages of Cu deposition onto a bare polycrystalline smooth Pt electrode from acidic $CuSO_4$ solution occur most likely through the instantaneous 3D nucleation and diffusion-controlled growth model proposed by Scharifker and Hills [41], simultaneously taking into account the different numbers of nuclei formed on different part of the area of working electrode surface. It was assumed that such parts should be of macroscopic dimensions rather than of microscopic or atomic ones.

Modification of the surface of polycrystalline Pt by adsorbed selenium species caused the mode of Cu deposition to change. For Cu deposition onto the Se-modified polycrystalline Pt electrode, the experimental current–time characteristics can be most likely interpreted on the basis of a model involving appreciable instantaneous 3D nucleation with diffusion-controlled growth onto one part of the working electrode, as with bare Pt, and only a negligible Cu deposition on the rest part corresponding likely to the selenium-covered Pt surface. Under conditions of our experiments with (Se)Pt, the first part of the electrode is larger in area, but the number of formed Cu nuclei per cm^2 is smaller than with bare Pt.

Received
2000
Accepted
10 January 2001

References

1. M. W. Breiter, *J. Electrochem. Soc*.,**114**, 1125 (1967).
2. G. Gunawardena, G. Hills and I. Montenegro, *J. Electroanal. Chem.*, **184**, 357 (1985).
3. D. Margheritis, R. C. Salvarezza, M. C. Giordano and A. J. Arvia, *J. Electroanal. Chem.*, **229**, 327 (1987).
4. M. H. Hölzle, V. Zwing and D. M. Kolb, *Electrochim. Acta,* **40**, 1237 (1995).
5. V. Karpavičienė and V. Kapočius, *Chemija (Vilnius)*, Nr. 2, 56 (1997).
6. A. I. Danilov, J. E. T. Andersen, E. B. Molodkina, Yu. M. Polukarov, P. Møller, and J. Ulstrup, *Electrochim. Acta*, **43**, 733 (1997).

7. A. B. Soto, E. Arce and I. Gonzalez, in *Abstr. 194th Meet. Electrochem. Soc.*, Vol. 98–2, Abstr. No. 25, Boston (1998).
8. M. H. Hölzle, C. W. Apsel, T. Will and D. M. Kolb, *J. Electrochem. Soc*., **142,** 3741 (1995).
9. R. Rashkov and C. Nanev, *J. Appl. Electrochem.*, **25**, 603 (1995).
10. A. Tarallo and L. Heerman, *J. Appl. Electrochem.*, **29**, 585 (1999).
11. M. Fleischmann and H. R. Thirsk, in *Advances in Electrochemistry and Electrochemical Engineering*, Vol. 3 (Ed. P. Delahay), Chapt. 3, Interscience Publishers, New York–London (1963).
12. A. I. Danilov and Yu. M. Polukarov, *Uspekhi Khimii,* **56**, 1082 (1987) (in Russian).
13. E. Budevski, G. Staikov and W. J. Lorenz, *Electrochemical Phase Formation and Growth,* VCH, Weinheim-New York–Basel–Cambridge–Tokyo (1996).
14. D. P. Bhatt, T. Twomey, W. Plieth, R. Schumacher and H. Meyer, *J. Electroanal. Chem.,* **322**, 279 (1992).
15. J. H. White and H. D. Abruña, *J. Electroanal. Chem.*, **300**, 521 (1991).
16. A. Steponavičius, S. Lichušina and D. Šimkūnaitė, in *Abstr. 2nd Baltic Conf. Electrochem.,* p. 147, Palanga (1999).
17. V. Karpavičienė and V. Kapočius, *Chemija (Vilnius)*, Nr. 1, 56 (1996).
18. C. Alonso, M. J. Pascual and H. D. Abruña, *Electrochim. Acta*, **42**, 1739 (1997).
19. A. Steponavičius and S. Lichušina, *Chemija (Vilnius)*, **10**(1), 36 (1999).
20. A. Steponavičius, S. Lichušina and D. Šimkūnaitė, *Chemija (Vilnius)*, (in press).
21. V. Karpavičienė, V. Kapočius and A. Steponavičius, *Chemija (Vilnius)*, Nr. 4, 31 (1997).
22. A. Steponavičius and V. Kapočius, in *Abstr. 1997 Joint Internat. Meet. Electrochem. Soc.& Internat. Soc. Electrochem.,* Abstr. Nr. 470, Paris (1997).
23. A. Steponavičius and D. Šimkūnaitė, *Chemija (Vilnius)*, Nr. 4, 297 (1998).
24. T. Loučka, *J. Electroanal. Chem.*, **31**, 319 (1971).
25. A. Q. Contractor and H. Lal, *J. Electroanal. Chem.*, **93**, 99 (1978).
26. T. Hemmingsen, *Electrochim. Acta*, **37,** 2775 (1992).
27. T. Hemmingsen, *Electrochim. Acta*, **37,** 2785 (1992).
28. C. Quijada, A. Rodes, J. L. Vázquez, J. M. Pérez and A. Aldaz, *J. Electroanal. Chem.*, **398**, 105 (1995).
29. N. Furuya and S. Motoo, *J. Electroanal. Chem.*, **98**, 189 (1979).
30. J. M. Feliu, R. Gómez, M. J. Llorca and A. Aldaz, *Surf. Sci.,* **289**, 152 (1993).
31. T. Biegler, D. A. J. Rand and R. Woods, *J. Electroanal. Chem.*, **29**, 269 (1971).
32. A. Steponavičius, D. Šimkūnaitė and S. Lichušina, *Chemija (Vilnius)*, (in press).
33. J. H. De Boer, in *Advances in Catalysis and Related Subjects,* Vol. 8 (Eds. W. G. Frankenburg, V. I. Komarewski and E. K. Rideal), Chapt. 2, IL, Moscow (1959) (in Russian).
34. P. J. Mitchell, N. A. Hampson, and A. J. S. McNeil, in *A Specialist Periodical Report. Electrochemistry*, Vol. 10. P. 1, The Royal Society of Chemistry, Burlington House, London (1985).
35. J. K. Foley, C. Korzeniewski, J. L. Daschbach and St. Pons, in *Electroanalytical Chemistry. A Series of Advances* (Ed. A. J. Bard), Vol. 14, p. 309, Marcel Dekker, Inc., New York–London (1986).
36. A. Steponavičius and L. Gudavičiūtė, *Chemija* (*Vilnius*) (in press).
37. Y. Shingaya, K. Hirota, H. Ogasawara and M. Ito, *J. Electroanal. Chem.*, **409**, 103 (1996).
38. M. Watanabe, H. Uchida and N. Ikeda, *J. Electroanal. Chem.*, **380**, 255 (1995).
39. S. Fletcher, *Electrochim. Acta,* **28**, 917 (1983).
40. V. Kapočius, V. Karpavičienė and A. Steponavičius, *Chemija* (*Vilnius*) (in press).
41. B. Scharifker and G. Hills, *Electrochim. Acta,* **28**, 879 (1983).
42. G. Gunawardena, G. Hills, I. Montenegro and B. Scharifker, *J. Electroanal. Chem.,* **138,** 225 (1982).
43. T. I. Quickenden and Q. Xu, *J. Electrochem. Soc.,* **143**, 1248 (1996).
44. G. Kokkinidis, C. Hasiotis and G. Papanastasiou, *J. Electroanal. Chem.*, **350**, 235 (1993).
45. M. Palomar-Pardavé, M. T. Ramirez, I. González, A. Serruya and B. R. Scharifker, *J. Electrochem. Soc.,* **143**, 1551 (1996).
46. A. Kelaidopoulou, G. Kokkinidis and A. Milchev, *J. Electroanal. Chem.,* **444**, 195 (1998).
47. A. Milchev, *J. Electroanal. Chem.,* **444**, 195 (1998).
48. H. Bort, K. Jüttner, W. J. Lorenz, G. Staikov and E. Budevski, *Electrochim. Acta,* **28**, 985 (1983).
49. B. R. Scharifker and J. Mostany, *J. Electroanal. Chem.,* **177**, 13 (1984).
50. V. Tsakova and A. Milchev, *J. Electroanal. Chem.,* **235**, 237 (1987).
51. R. L. Deutscher and S. Fletcher, *J. Electroanal. Chem.,* **239**, 17 (1988).
52. A. Milchev, W. S. Kruijt, M. Sluyters-Rehbach and J. H. Sluyters, *J. Electroanal. Chem.,* **362**, 21 (1993).
53. M. E. Martins, R. C. Salvarezza and A. J. Arvia, *Electrochim. Acta,* **41**, 2441 (1996).
54. E. B. Budevski, in *Comprehensive Treatise of Electrochemistry,* Vol. 7 (Eds. B. E. Conway, J. O'M. Bockris, E. Yeager, S. U. M. Khan, and R. E. White), Ch. 7(A), Plenum Press, New York–London (1983).
55. A. Milchev, V. Tsakova, T. Chierche, K. Jüttner and W. J. Lorenz, *Electrochim. Acta,* **31**, 971 (1986).
56. L. D. Burke and A. P. O'Mullane, *J. Solid State Electrochem.,* **4**, 285 (2000).
57. D. M. Kolb, in *Advances in Electrochemistry and Electrochemical Engineering,* Vol. 11 (Eds. H. Gerischer and Ch. W. Tobias), p. 125, John Wiley & Sons, New York–Chichester–Brisbane–Toronto (1978).
58. J. W. Schultze, *Ber. Bunsenges. Physik. Chem.*, **74**, 705 (1970).
59. B. J. Bowles, *Electrochim. Acta,* **15**, 589 (1970).
60. J. S. Hammond and N. Winograd, *J. Electroanal. Chem.,* **80**, 123 (1977).
61. C. L. Scortichini and Ch. N. Reilley, *J. Electroanal. Chem.,* **139**, 233 (1982).
62. C. L. Scortichini and Ch. N. Reilley, *J. Electroanal. Chem.,* **139**, 247 (1982).
63. C. L. Scortichini, F. E. Woodward and Ch. N. Reilley, *J. Electroanal. Chem.,* **139**, 265 (1982).

64. V. Karpavičienė and V. Kapočius, *Chemija (Vilnius),* Nr. 4, 15 (1993) (in Russian).
65. M. R. H. Hill and G. T. Rogers, *J. Electroanal. Chem.,* **68**, 149 (1976).
66. T. I. Lezhava, *Acceleration at Deposition of Metals,* Diss., A. Frumkin Inst. Electrochem., Moscow (1979) (in Russian).
67. D. Šimkūnaitė and A. Steponavičius, *Chemija (Vilnius)*, Nr. 1, 16 (1994).
68. S. Lichušina, D. Šimkūnaitė, A. Steponavičius and P. Miečinskas, *Chemija (Vilnius)*, Nr. 4, 29 (1996).
69. A. Steponavičius, D. Šimkūnaitė and A. Survilienė, *Chemija (Vilnius)*, Nr. 3, 36 (1997).
70. A. Steponavičius, D. Šimkūnaitė and V. Kapočius, *Chemija (Vilnius)*, Nr. 4, 40 (1997).
71. J. Mostany, J. Mozota and B. R. Scharifker, *J. Electroanal. Chem.,* **177**, 25 (1984).
72. J. Shin-Yu and I.-W. Sun, *J. Electrochem. Soc*., **144**, 140 (1997).
73. V. Tsakova and A. Milchev, *J. Electroanal. Chem.,* **197**, 359 (1986).
74. R. K. Pandey, S. N. Sahu and S. Chandra, *Handbook of Semiconductor Electrodeposition,* Marcel Dekker, Inc., New York–Basel–Hong Kong (1996).

A. Steponavičius, D. Šimkūnaitė, S. Lichušina ir V. Kapočius

KAI KURIŲ PRIEDŲ ĮTAKA Cu SLUOKSNIŲ FORMAVIMUISI POTENCIALŲ ZONOSE, TEIGIAMESNĖSE IR NEIGIAMESNĖSE UŽ PUSIAUSVYRINĘ SISTEMOS Cu^{2+}/Cu^{o} POTENCIALO REIKŠMĘ, RŪGŠČIUOSE $CuSO_4$ TIRPALUOSE 7. Cu BRANDUOLIŲ UŽUOMAZGŲ SUSIDARYMAS IR AUGIMAS ANT GLOTNAUS POLIKRISTALINIO Pt IR ANT Se MODIFIKUOTO Pt ELEKTRODŲ

S a n t r a u k a

Ciklinės voltamperometrijos ir potenciostatinio įjungimo metodais buvo tirtos Cu nusodinimo pirmosios stadijos ant švaraus ir ant selenu modifikuoto glotnaus polikristalinio Pt elektrodo 0,5 M H_2SO_4 + 0,1 M $CuSO_4$ tirpale. Nustatyta, kad esant potencialams, neigiamesniems už poros Cu^{2+}/Cu^{o} pusiausvyrinį potencialą, Cu nusodinimo pirmosios stadijos ant švaraus Pt elektrodo, matyt, vyksta pagal momentinio 3D branduolių užuomazgų susidarymo ir difuzijos kontroliuojamo augimo modelį, pasiūlytą Scharifker ir Hills, atsižvelgiant į susidariusių užuomazgų skirtingą skaičių įvairiose elektrodo paviršiaus vietose. Padaryta prielaida, kad tokios paviršiaus vietos yra greičiau makroskopinių matmenų, negu mikroskopinių ar atominių.

Ant modifikuoto adsorbuotu selenu Pt paviršiaus Cu nusodinimo pobūdis kinta. Potenciostatinės „srovė–laikas“ priklausomybės, gautos nusodinus Cu ant Se modifikuoto Pt elektrodo, gali būti interpretuojamos remiantis modeliu, pagal kurį ant dalies Pt elektrodo paviršiaus branduolių užuomazgų susidarymas yra momentinis, kaip švarios Pt atveju, ir, priešingai, ant likusios elektrodo dalies, matyt, padengtos selenu, branduolių užuomazgos susidaro progresuojančiai. Nors pirmosios elektrodo paviršiaus dalies plotas yra didesnis, susidariusių Cu užuomazgų skaičius ploto vienetui yra mažesnis, negu su švaria Pt.

Pt elektrodo potencialo kitimas po įvairios trukmės potencialo impulso foniniame 0,5 M H_2SO_4 tirpale parodė, kad švarios Pt ir Se modifikuotos Pt potencialų kitimas laikui bėgant yra skirtingas.

А. Степонавичюс, Д. Шимкунайте, С. Лихушина, В. Капочюс

ВЛИЯНИЕ НЕКОТОРЫХ ДОБАВОК НА ФОРМИРОВАНИЕ Cu В ЗОНАХ НЕДОНАПРЯЖЕНИЯ И ПЕРЕНАПРЯЖЕНИЯ В КИСЛЫХ РАСТВОРАХ $CuSO_4$ 7. ЗАРОДЫШЕОБРАЗОВАНИЕ И РОСТ Cu КРИСТАЛЛОВ НА ГЛАДКОЙ ПОЛИКРИСТАЛЛИЧЕСКОЙ Pt И НА Se-МОДИФИЦИРОВАННОЙ Pt

Р е з ю м е

Методами циклической вольтамперометрии и потенциостатического включения исследовали начальные стадии осаждения Cu на гладкой поликристаллической Pt и на Se-модифицированной Pt в растворе 0,5 M H_2SO_4 + 0,1 M $CuSO_4$. Установлено, что при потенциалах, более отрицательных, чем равновесное значение для системы $Cu^{2+}/Cu°$, первые стадии осаждения Cu на чистой Pt, по всей вероятности, происходят по модели 3D зародышеобразования и диффузией контролируемого роста, предложенной Шарифкером и Хиллсом, с учетом того, что число образовавшихся зародышей в разных местах поверхности электрода может быть неодинаковым. Высказано предположение, что эти места на поверхности электрода имеют скорее макроскопические размеры, чем микроскопические или атомные.

На поверхности Pt электрода, модифицированного селеном, характер осаждения Cu изменяется. Потенциостатические „ток-время“ кривые, полученные при осаждении Cu на Se-модифицированной Pt, могут быть интерпретированы с использованием модели, согласно которой на одной части поверхности электрода зародышеобразование является моментным, как в случае чистой Pt, но, в противоположность, на остальной части поверхности, по-видимому, покрытой селеном, зародышеобразование является прогрессирующим. Хотя площадь первой части поверхности электрода является большей, число образовавшихся зародышей на $см^2$ является меньшим по сравнению с чистой Pt.

Установлено, что после прекращения поляризации характер изменения потенциалов чистой Pt и Se-моди фицированной Pt во времени является довольно разным.